

**NASA
Technical
Paper
2798**

March 1988

**Laser Production and
Heating of Plasma
for MHD Application**

p. 11

N. W. Jalufka

(NASA-TP-2798) LASER PRODUCTION AND HEATING
OF PLASMA FOR MHD APPLICATION (NASA) 11 p
CSCL 201

N88-18443

Unclas
H1/75 0128136

NASA

**NASA
Technical
Paper
2798**

1988

Laser Production and Heating of Plasma for MHD Application

N. W. Jalufka

*Langley Research Center
Hampton, Virginia*



National Aeronautics
and Space Administration

Scientific and Technical
Information Division

Introduction

The development of a space-based transmission system that will utilize high-power lasers as transmitters will require not only efficient laser systems but also efficient converter systems to convert the laser energy into a more useful form such as electricity. The characteristics desirable for such a converter are as follows:

1. Wavelength independence
2. High energy-conversion efficiency
3. High power density
4. High power-to-weight ratio
5. Reliable and maintenance-free operation
6. Not excessively expensive to manufacture

Wavelength independence is desirable so that any available laser may be utilized. Visible wavelengths are more desirable than infrared because of their better transmission and conversion properties. Smaller beam divergence of visible wavelengths is important in reducing the size of the transmitting and receiving optics, whereas the larger photon energy is more easily matched to proposed photovoltaic receivers. High energy-conversion efficiency and high power density operation are closely related. The need for high energy-conversion efficiency is required since transmitted energy that is not converted to a useful form will be converted to heat which must be rejected from the system. High power-to-weight ratio will minimize the system weight for a given power capacity, which, in turn, will minimize launch weight and cost. Characteristics 5 and 6 are self-evident. Three concepts that may satisfy these converter characteristics are optical rectification, laser-driven magneto-hydrodynamics (MHD), and reverse free-electron laser. These devices are shown in figure 1.

Although optical rectification (ref. 1) and the reverse free-electron laser offer the potential of meeting the above characteristics, the technology base for these two concepts is extremely limited. The laser-driven magnetohydrodynamic generator, on the other hand, has available for its development a wealth of experimental and theoretical data on MHD generating systems and laser-plasma interaction phenomena. Coupling of the two concepts is straightforward and development would proceed at a fairly rapid pace.

Over the past few years, experiments have been carried out at the Langley Research Center in order to assess the potential of a laser-driven MHD generator as a power converter. These experiments were designed to study the laser-plasma interaction specifically, and, in particular, the absorption of laser energy by the plasma as well as the extraction of the

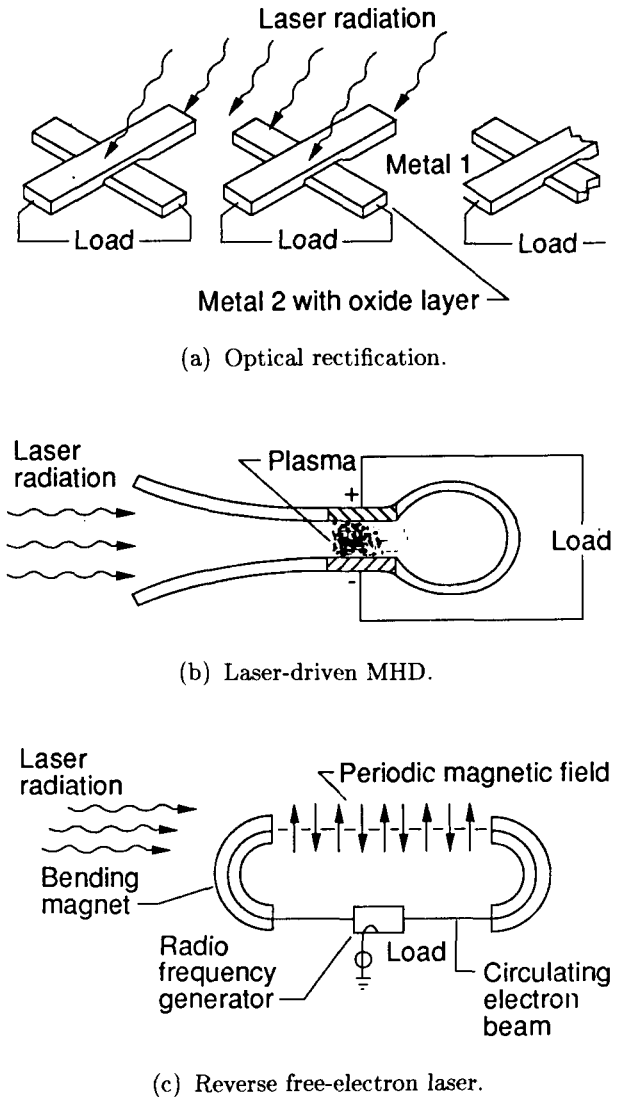


Figure 1. Three concepts for laser converters.

energy from the flowing plasma by use of an MHD generator.

Plasma Heating With a Laser

Heating of a plasma by absorption of laser energy occurs by inverse bremsstrahlung whereby the laser radiation is absorbed by free electrons. The electrons will then transfer energy to ions and neutral atoms by collisions. The absorption coefficient α for inverse bremsstrahlung is given by (ref. 2)

$$\alpha = \frac{(7.8 \times 10^{-9}) Z_i n_e^2 \ln \Lambda(\nu)}{\nu^2 T_e^{3/2} \left(1 - \frac{\nu_p^2}{\nu^2}\right)^{1/2}} \quad [\text{cm}^{-1}] \quad (1)$$

where Z_i is the ionic charge, n_e is the electron density in cm^{-3} , Λ is the high-frequency screening

parameter, T_e is the electron temperature in eV, ν is the laser frequency, and ν_p is the plasma frequency. Coupling of the laser energy into the plasma is most efficient if the electron density of the plasma is such that ν_p is close to ν so that the absorption depth α^{-1} is a minimum. For plasmas of interest in MHD systems, electron densities are in the range from 10^{16} to 10^{17} cm^{-3} . The corresponding absorption depths (for $T_e = 1.0 \text{ eV}$) are 200 cm and 2 cm, respectively. If the electron density of the plasma reaches a density for which $\nu_p = \nu$, the absorption coefficient becomes infinite and the laser beam does not penetrate into the plasma. The critical density n_c is given by (ref. 3)

$$n_c = (1.24 \times 10^{-8}) \nu^2 \quad (2)$$

For the $10.6\text{-}\mu\text{m}$ radiation produced by the CO_2 laser, this critical density is approximately 10^{19} cm^{-3} . This situation results in a laser-supported detonation (LSD) wave propagating from the plasma surface along the laser beam toward the laser. These waves move at supersonic speeds and ionize and heat the medium through which they are propagating.

The energy absorbed by the free electrons can be dissipated in several ways: (1) expansion of the plasma volume; (2) heating of the electrons, ions, and neutral atoms; (3) inelastic collision resulting in excitation and ionization of the ions and atoms; (4) diffusion of electrons out of the plasma; (5) attachment of electrons to atoms to form negative ions; and (6) radiative losses such as bremsstrahlung and radiative recombination. The relative importance of these various processes depends on the plasma parameters, and in many cases some of the processes are negligible. For efficient MHD power generation, the important processes are expansion of the plasma volume and heating of the electrons which, at the pressure and temperatures applicable here ($n_e \approx 10^{16}$ to 10^{17} cm^{-3} , $T_e \approx 0.5$ to 1.0 eV), are shown to dominate; the other processes represent energy losses, with radiative recombination being the major loss mechanism (ref. 4).

The increase in electron temperature due to absorption of laser energy $\Delta T_e/T_e$ is given by (ref. 5)

$$\frac{\Delta T_e}{T_e} = (1.42 \times 10^{25}) \frac{n_i Z_i^2 g_{ff}}{T_e^{3/2} \nu^3} \left[1 - \exp\left(\frac{h\nu}{T_e}\right) \right] \frac{1}{q} \int_0^{t_L} L dt \quad (3)$$

where n_i is the ion density in cm^{-3} , g_{ff} is the free-free gaunt factor, T_e is in eV, h is Planck's constant, q is the cross section of the laser beam in cm^2 , t_L is

the laser pulse length in seconds, and L is the laser intensity.

If the plasma exists for an adequate length of time, the electrons will transfer energy to the ions by collision, and for a Coulomb-dominated plasma, equilibrium is reached in a time t_{eq} given (in seconds) by (ref. 6)

$$t_{eq} = (7.34 \times 10^6) \frac{A_e A_f}{n_f Z_e^2 Z_i^2 \ln \Lambda} \left(\frac{T_e}{A_e} + \frac{T_i}{A_i} \right)^{3/2} \quad (4)$$

where A_e is the atomic weight of the particle, the subscript i refers to the field (heavier) particle, and the subscript e refers to electrons. For electrons $Z_e = 1$ and in the plasmas investigated here, only single ionization occurred with the result that Z_i was also equal to 1.

Experiments With a Large CO_2 Laser

Laser. The laser used in the first experiments was a large pulsed CO_2 system consisting of an oscillator and an amplifier. The system was a conventional transverse electric, atmospheric (TEA) pressure design with an unstable resonator operated on a $\text{He:N}_2:\text{CO}_2$ (8:1:1) mixture with a repetition rate of 1 Hz. The peak energy output was 100 J with a pulse width of 80 nsec full width at half maximum (FWHM) intensity.

Test chamber. Figure 2 is a schematic of the experimental arrangement. The laser beam was focused by a germanium (Ge) lens to a rectangular spot 1 cm by 2 cm at the center of the test chamber. The test chamber was a 5-cm inside-diameter (I.D.) Corning Pyrex T-shaped tube with germanium windows. The test chamber was normally filled with argon gas, generally at atmospheric pressure but with some tests conducted at a lower pressure. The spectrograph was a 0.5-m Czerny-Turner mount that could be equipped with a photomultiplier tube and used as a monochromator. The streak camera was used to measure the velocity of the LSD wave propagating from the focal point of the lens toward the laser. For this measurement, the test chamber walls were completely covered with black tape except for a 1-mm-wide horizontal slit. An image of this slit was formed on the photocathode of the streak camera. When the camera was triggered, the slit image was deflected in the vertical direction as a function of time. The resulting data are illustrated in figure 3. The slope of the line gives the velocity of the LSD wave (i.e., $\Delta X/\Delta T$). Measured values of the velocity were typically between 10^6 and 10^7 cm/sec . (Sound velocity in hydrogen is $1.284 \times 10^5 \text{ cm/sec}$.)

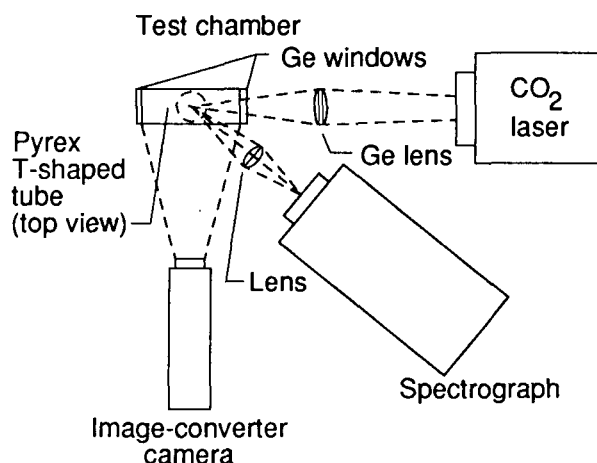


Figure 2. Schematic of experimental arrangement.

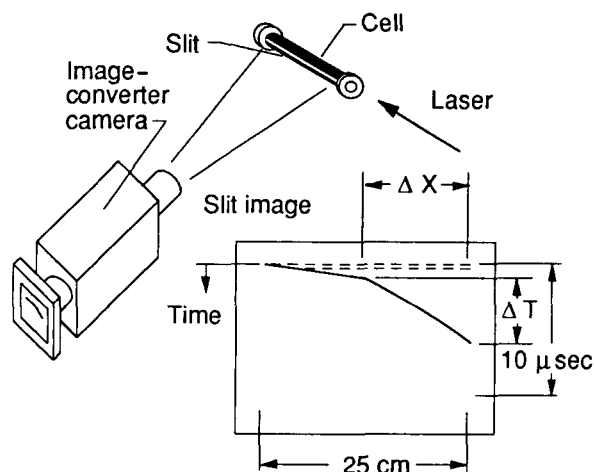


Figure 3. Measurement of LSD wave velocity.

The emission from the plasma was recorded using the 0.5-m spectrograph. The spectrum, in the visible region, was recorded on film, and the wavelength of the emission lines was determined by comparison to the mercury spectrum. The spectrum was dominated by singly and doubly ionized argon lines that appear in this type of plasma at temperatures between 1 and 2 eV. The LSD wave was initiated when ionization in the plasma (created in the test chamber) became sufficient so that the plasma frequency ν_p was equal to the laser frequency ν . For the $10.6\text{-}\mu\text{m}$ CO_2 radiation, this occurs at $n_e \approx 10^{19} \text{ cm}^{-3}$.

Although this system worked well and produced consistent results, it was not the most convenient for studying plasma heating by lasers since the plasma is produced and heated by the laser simultaneously. Consequently, this system was replaced by a

system consisting of a shock tube to produce a dense, low-temperature plasma that was then heated by a smaller CO_2 laser. This arrangement allowed separation of the heating phenomena from the actual production phase of the plasma.

Experiments With a Shock Tube and Laser

Laser. The laser used in this investigation was a small, pulsed, commercial TEA CO_2 laser with a stable resonator operated at atmospheric pressure. The pulse width and energy per pulse could be varied by varying the gas mixture, which was typically $\text{He:N}_2:\text{CO}_2$ (8:1:1). The laser output energy was 1 J with a pulse width of 80 nsec (FWHM).

Shock tube. The plasma was produced in a T-type, electromagnetic shock tube. The side arm of the tube (fig. 4) was commercial glass tubing with a 2.5-cm inside diameter. The distance from the electrodes to the observation area was 50 cm. Hydrogen was used as the fill gas at pressures in the range from 1 to 5 torr. The discharge was powered by a $12.5\text{-}\mu\text{F}$ capacitor, which could be charged to 20 kV but was normally operated at 12.5 kV (976 J). The system had a ringing frequency of 50 kHz. The shock tube was connected to an aluminum housing (fig. 5) that had eight observation ports, an adjustable reflector, and a pumping port through which the system could be evacuated (base pressure 1.0×10^{-6} torr) and the gas introduced. The observation windows were quartz, except for those through which the laser beam passed which were NaCl.

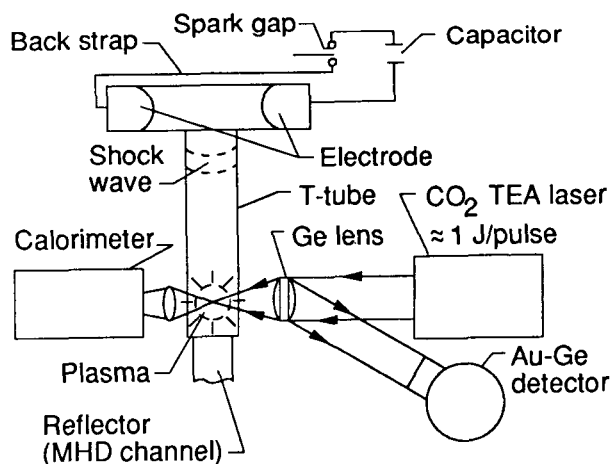


Figure 4. T-type electromagnetic shock tube.

Experiment setup. A general schematic of the experimental arrangement is shown in figure 5. The

laser beam was focused by a germanium lens (20-cm focal length) to a spot size 1 mm by 2 mm at the tube axis. The laser output power was monitored by a gold-doped germanium detector (Au-Ge detector), and the laser energy transmitted through the plasma was measured with a calorimeter. Two monochromators were used for spectroscopic measurements. Both instruments were 25-cm focal-length Ebert mount with 1200 lines per millimeter gratings. Both instruments were equipped with S-20 phototubes and were calibrated for absolute intensity using a standard carbon arc according to Lochte-Holtgreven and Richter (ref. 7). The wavelength drives were calibrated using a low-pressure mercury lamp. One of the monochromators measured the absolute intensity of the hydrogen alpha (H_α) line, whereas the other measured the absolute intensity of a 100-Å band of adjacent continuum. A scanning Fabry-Perot interferometer was also used to scan the profile of a silicon (Si) impurity line (4130.9 Å Si II). The interferometer had 5.0-cm-diameter mirrors, a free spectral range of 5.69 Å, a finesse of 20, and a scan time of 0.41 Å/μsec.

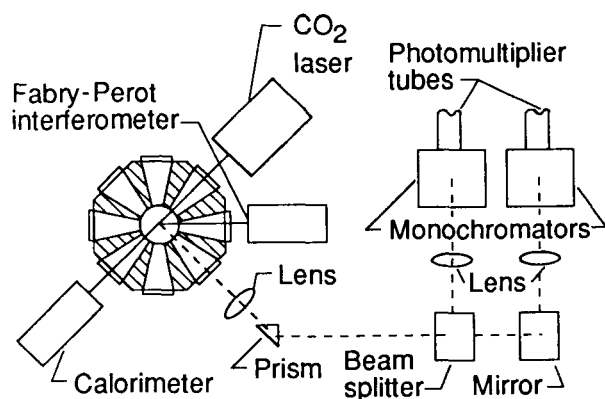


Figure 5. Laser-heated plasma.

Diagnostic Measurements

Diagnostic measurements of the plasma produced by the shock tube without laser heating were made spectroscopically. Preliminary measurements of the electron density were obtained by scanning the Stark-broadened H_α line shot-to-shot while monitoring the total intensity of the continuum band. Comparison of the measured profile with theoretical profiles (ref. 8) established a range of electron densities that could be obtained in the shock tube. This also established the shot-to-shot reproducibility of the shock tube (± 20 percent). On each run, the data obtained consisted of the absolute intensity of H_α , the absolute intensity of the adjacent continuum, and the Stark-broadened width of the silicon impurity line. These

data were used as input for computation of the electron temperature from the line to continuum ratio, the electron density from the absolute continuum intensity, a second value for electron density from the Stark-broadened width of the silicon impurity line, and a second value of the electron temperature from the absolute intensity of the H_α line. These values were then compared with values of n_e and T_e calculated from the Saha equation, which is based on local thermodynamic equilibrium (LTE), and agreed within an experimental uncertainty of ± 15 percent. Figures 6 and 7 show the electron density and the electron temperature, respectively, as a function of time for a typical run.

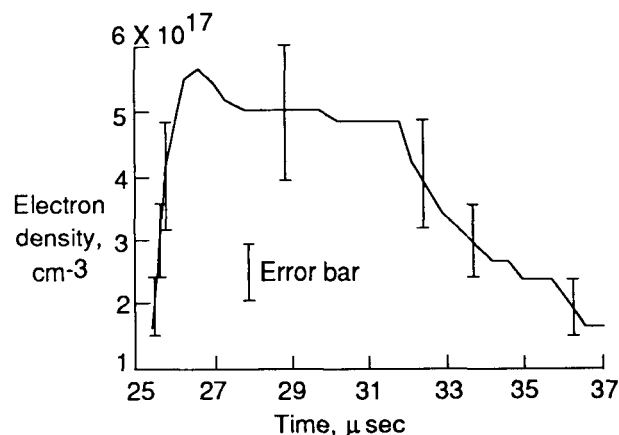


Figure 6. Electron density plotted against time for electromagnetic shock tube.

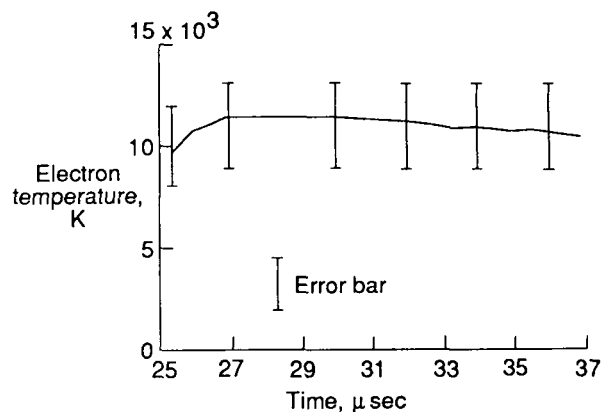


Figure 7. Electron temperature plotted against time for electromagnetic shock tube.

Absorption of the CO_2 laser beam was investigated by measurement of the beam energy transmitted through the plasma. The delay in firing the laser

was increased in steps of 1 μsec (0.5 μsec at peak absorption), and five measurements were made at each time setting. Figure 8 shows the absorption as a function of time and indicates that a dense plasma exists in the observation area for times up to 100 μsec . After this time, the plasma is low enough in density that the absorption depth for the laser radiation is much larger than the plasma dimension (approximately 3 to 4 cm).

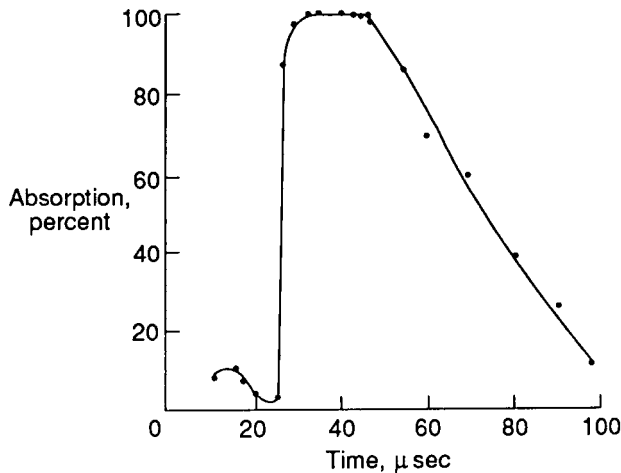


Figure 8. Absorption of CO_2 laser radiation by shock-tube plasma plotted against time.

Validity of Spectroscopic Measurements

The validity for the methods used to obtain the most probable electron density and electron temperature depends on the establishment of local thermodynamic equilibrium in the plasma, a condition requiring that the collision rates exceed the radiative rates in the plasma. Conditions for the establishment of LTE in transient plasmas are given by McWhiter (ref. 9) for electron density and by Griem (ref. 8) for ionization relaxation times.

The optically thick condition is satisfied if (ref. 8)

$$nd \gg \frac{(1.1 \times 10^9)}{f\lambda'} \frac{T_e^{1/2}}{A} \quad [\text{cm}^{-2}] \quad (5)$$

where n is the density of the ion stage of the atom from which the spectral line originates, d is the plasma dimension in cm, f is the absorption oscillator strength, A is the atomic weight, and λ' is the wavelength of the resonance line in cm. The optically thick condition is met in a 2-cm-long plasma for both hydrogen and silicon at densities greater than 10^{12} cm^{-3} .

In order for LTE to exist in an optically thick and collision-dominated plasma, the requirement for the electron density is given as (ref. 8)

$$n_e \geq (1.6 \times 10^2) \chi^3 T_e^{1/2} \quad [\text{cm}^{-3}] \quad (6)$$

where χ is the excitation energy of the resonance line in eV and T_e is in eV. If the plasma is optically thin, the density must be an order of magnitude higher. The ionization relaxation time τ (the time required for the ionization to reach a steady-state value) must be shorter than the plasma lifetime. The expression for τ is (ref. 8)

$$\tau = \frac{(1.5 \times 10^7) N^+ \chi T_e^{1/2}}{f n_e (N^+ + N) (13.6)^{3/2}} \exp\left(\frac{\chi}{T_e}\right) \quad [\text{sec}] \quad (7)$$

where N and N^+ are the neutral and ion densities, respectively. The ionization relaxation times are of the order of 10^{-8} sec . According to equation (6), a density of $n_e = (2 \times 10^{15}) \text{ cm}^{-3}$ is required for LTE to be established. Measured densities were generally in the 10^{17} cm^{-3} range so that the criterion for LTE was easily met.

Plasma Heating by Laser

Measurements of electron temperature and electron density were obtained continuously as a function of time on each run. This allowed measurements to be made before and after the laser was fired. The time delay between firing the shock tube and firing the laser was varied over a time span of approximately 150 μsec corresponding to the lifetime of the plasma. This time increment (delay) was normally 5 μsec when the plasma was decaying slowly and 1 μsec when the change was rapid. Figure 9 shows a typical signal from the two monochromators with the laser being fired near the peak of the emission. The rapid change in intensity and the electrical noise generated when the laser was fired prevented any accurate measurements over the time interval of several microseconds. Consequently, the detailed behavior of the plasma during the period of absorption is not known. For the data presented, the measurements show an increase in electron temperature of 16 percent.

The measured increase in the plasma temperature was compared with values calculated from equation (3). The measured temperature increase was less than that expected assuming all the absorbed energy was utilized in heating the plasma. The remaining absorbed energy was assumed to go into expansion

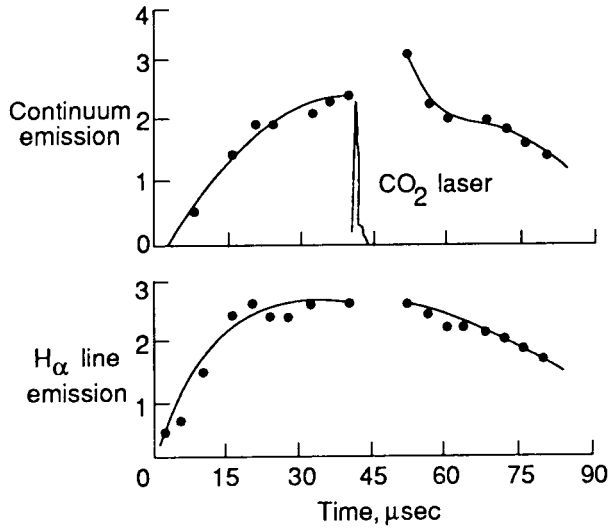


Figure 9. Total line and continuum emission plotted against time with laser heating.

of the gas (ref. 10), and no attempt was made to investigate this assumption.

Experiments With an MHD Generator

Power may be extracted from a moving plasma by use of an MHD generator. This concept has existed since the time of Faraday, and considerable research and development have been carried out in this area with the result that several large terrestrial systems are now in operation around the world (ref. 11). The concept of using an MHD system as a laser-to-electrical power converter is attractive since high absorption of the laser beam by a plasma (approximately 100 percent) can be achieved as demonstrated here (refs. 12 and 13) and the MHD generator exhibits a high conversion efficiency (approximately 70 percent) (ref. 14).

An MHD generator consists of a conductor moving through a fixed magnetic field. In these systems the conductor is a high-temperature ionized gas (plasma) or a liquid metal. Electrical current I is extracted from the flowing plasma by electrodes. Figure 10 is a schematic of the simple MHD generator used in the experiments reported herein. Power output was determined by measuring the voltage across a 1-M Ω resistor (R) on an oscilloscope. The voltage is just the IR product, and since R was known the current I could be determined. The power was then calculated as I^2R .

In order to determine if the laser energy absorbed by the plasma could be efficiently extracted as

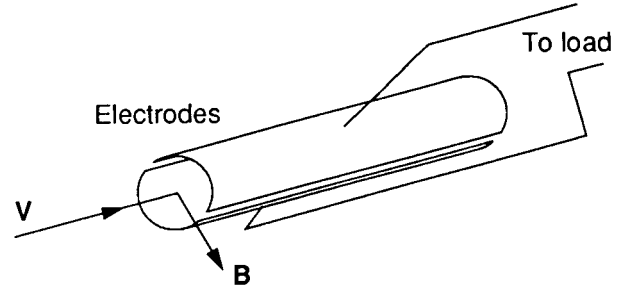


Figure 10. Simple MHD generator used in experiments.

electrical energy, a simplified Hall-type MHD generator was constructed and installed on the T-tube in place of the end assembly. The magnetic field was supplied by a permanent magnet with a field strength of 4.5 kilogauss between the pole faces. Figure 11 shows the MHD generator arrangement. The generator was constructed from 2-cm outside-diameter (O.D.) quartz tubing that was 12 cm long. The electrodes were constructed of aluminum and were 1.5 cm wide and 5 cm long. The power equation for such a Hall generator is given by (ref. 15)

$$P = \frac{\beta^2}{1 + \beta^2} \sigma V^2 B^2 K(1 - K) \quad (8)$$

where β is the ratio of the electron mean free path to the Larmor radius, σ is the plasma conductivity, V is the flow velocity, B is the magnetic field, and K is the ratio of load to open-circuit voltage. If the plasma is in the Coulomb-dominated regime, σ is proportional to $T^{3/2}$ (refs. 6 and 14), so that increasing the temperature increases the power output of the generator. If the laser energy is deposited in a short time, the rapidly heated gas also expands, thus increasing V and, consequently, the generator output.

During the course of the investigation, the delay time between the arrival of the initial shock wave at the entrance to the MHD generator and the firing of the laser was increased in 1- μ sec steps. Several runs were made at early delay times (less than the time for the shock wave to travel the length of the tube), and average values of the power (extracted from plasmas not heated by the laser) were determined.

For delay times of 25 to 50 μ sec, absorption up to 100 percent was observed (see fig. 8), but little change in the generator output was observed. However, for delay times greater than 50 μ sec, less absorption occurred, but a significant increase in the generator output was observed. Figure 12 shows the generator output with and without laser heating at 90- μ sec delay (maximum measured extraction). At

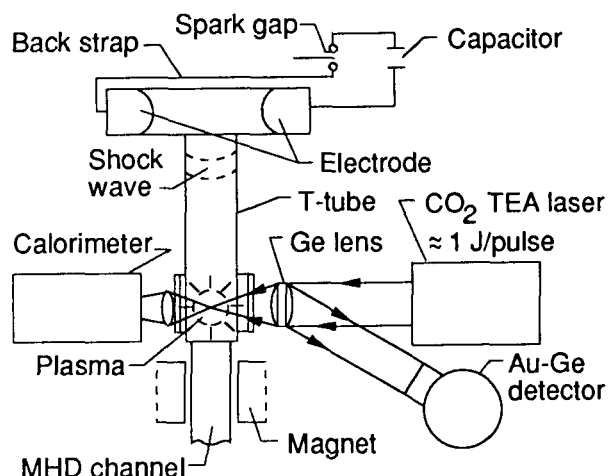


Figure 11. T-tube experimental arrangement of MHD generator.

this time, the electron temperature had fallen to 5000 K and the electron density to approximately 10^{15} cm^{-3} . The absorption of the laser beam was approximately 25 percent, which was still adequate to heat the plasma and increase its electron density. The extraction efficiency is defined as the ratio of the power output of the generator due to the laser heating (i.e., integrated power out with laser divided by integrated power out without laser) to the laser power absorbed. The highest value obtained (at 90- μsec delay) was 56 percent. Figure 13 shows the extraction efficiency as a function of delay time. The error bars represent the shot-to-shot variation in the experiment.

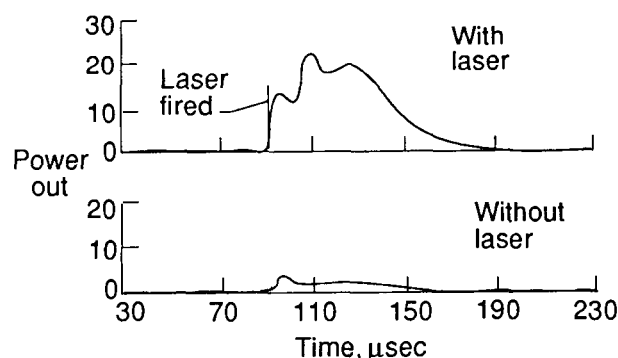


Figure 12. Output of MHD generator both with and without laser heating.

Results and Discussion

Although the experiments conducted were not exhaustive, the results (to be described below) strongly

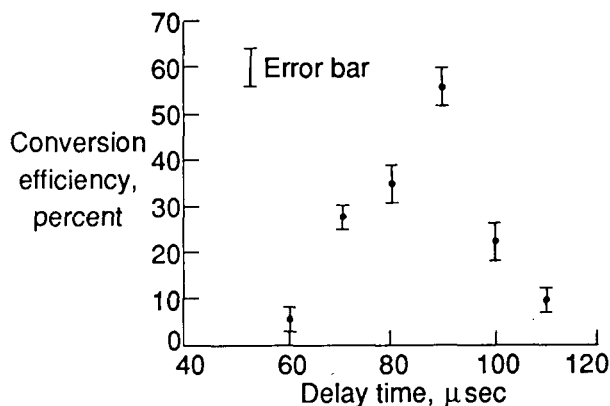


Figure 13. Conversion efficiency plotted against delay time.

suggest that a laser-driven MHD converter system is a viable option for space power transmission. These results are in agreement with previous studies by the author (ref. 16).

The experiment with the CO_2 laser, which both produced a plasma and heated it, suggests that pulsed laser-driven MHD generators operating with LSD waves are a definite possibility. It demonstrates that the plasma electron density can reach a critical value resulting in the formation and backward propagation of an LSD wave at a velocity between 10^6 and 10^7 cm/sec . Peak electron temperatures of 1 to 2 eV were estimated for this plasma based on the emission spectrum. These values of T_e and n_e suggest that a very efficient laser-driven MHD converter system could be based on this concept. In fact, this system has been studied theoretically by Maxwell and Myrabo (ref. 17) who concluded that efficiencies approaching 50 percent are possible.

The experiments with the laser-heated shock-tube plasma demonstrated conclusively that absorption of the laser beam by a plasma can be very efficient (>90 percent) and that, under certain conditions, extraction of this energy by an MHD generator is very efficient with values up to 56 percent measured in these experiments.

The low extraction efficiency measured during the initial phase of the plasma flow is not understood. Absorption of the laser beam may have introduced turbulence into the flow. If this is the case, some limit will be imposed on the amount of energy per unit volume that can be added to the flow. This restriction certainly would apply to a pulsed system and also present a limitation to a continuous system.

Concluding Remarks

Experiments have been made to study the absorption of laser radiation by a plasma and the

conversion of this absorbed energy to electrical power by a magnetohydrodynamic (MHD) generator. The large amount of absorption observed in this experiment, along with the high extraction efficiency measured with the MHD generator, suggests that these methods have considerable potential as a laser-to-electricity converter. Such a system would have several advantages:

1. Wavelength independence
2. High energy-conversion efficiency
3. High power density
4. High power-to-weight ratio
5. Reliable and maintenance-free operation

The results of these experiments strongly suggest that further research be carried out in this area in order to ascertain fully the potential of these laser-driven MHD systems.

NASA Langley Research Center
Hampton, Virginia 23665-5225
February 8, 1988

References

1. Twu, Bor-long; and Schwarz, S. E.: Mechanism and Properties of Point-Contact Metal-Insulator-Metal Diode Detectors at $10.6\ \mu$. *Appl. Phys. Lett.*, vol. 25, no. 10, Nov. 15, 1974, pp. 595-598.
2. Johnston, Tudor Wyatt; and Dawson, John M.: Correct Values for High-Frequency Power Absorption by Inverse Bremsstrahlung in Plasmas. *Phys. Fluids*, vol. 16, no. 5, May 1973, p. 722.
3. Key, M. H.: Interactions of Intense Laser Radiation With Plasma. *Philos. Trans. Royal Soc. London*, vol. A300, no. 1456, Apr. 23, 1981, pp. 599-612.
4. DeCoste, R.; Englehardt, A. G.; Fuchs, V.; and Neufeld, C. R.: Transverse Heating of a Cold Dense Helium Plasma by a Pulsed CO_2 Laser Beam. *J. Appl. Phys.*, vol. 45, no. 3, Mar. 1974, pp. 1127-1134.
5. Kunze, H. J.: The Laser as a Tool for Plasma Diagnostics. *Plasma Diagnostics*, W. Lochte-Holtgreven, ed., North-Holland Publ. Co., 1968, pp. 550-616.
6. Spitzer, Lyman, Jr.: *Physics of Fully Ionized Gases*, Second rev. ed. Interscience Publ., c.1962.
7. Lochte-Holtgreven, W.; and Richter, J.: Quantitative Spectroscopy and Spectral Photometry. *Plasma Diagnostics*, W. Lochte-Holtgreven, ed., John Wiley & Sons, Inc., 1968, pp. 250-346.
8. Griem, Hans R.: *Plasma Spectroscopy*. McGraw-Hill Book Co., c.1964.
9. McWhiter, R. W. P.: Spectral Intensities. *Plasma Diagnostic Techniques*, Richard H. Huddleston and Stanley L. Leonard, eds., Academic Press Inc., 1965, pp. 201-264.
10. Box, S. J. C.; John, P. K.; and Byszewski, W. W.: Interaction of a CO_2 Laser Beam With a Shock-Tube Plasma. *J. Appl. Phys.*, vol. 48, no. 5, May 1977, pp. 1946-1952.
11. Grundy, Robert F., ed.: *Magnetohydrodynamic Energy for Electric Power Generation*. Noyes Data Corp., 1978.
12. Jalufka, N. W.; and Kloc, Barbara J.: Interaction of CO_2 Laser Radiation With a Shock-Heated Hydrogen Plasma. *Bull. American Phys. Soc.*, vol. 30, no. 2, Feb. 1985, p. 138.
13. Lee, Ja H.; McFarland, Donald R.; and Hohl, Frank: Production of Dense Plasmas in a Hypocycloidal Pinch Apparatus. *Phys. Fluids*, vol. 20, no. 2, Feb. 1977, pp. 313-321.
14. Sutton, George W.; and Gloersen, Per: Magnetohydrodynamic Power and Propulsion. *Magnetohydrodynamics*, Ali Bulent Cambel, Thomas P. Anderson, and Milton M. Slawsky, eds., Northwestern Univ. Press (Evanston, Ill.), c.1962, pp. 243-268.
15. Sutton, George W.; and Sherman, Arthur: *Engineering Magnetohydrodynamics*. McGraw-Hill Book Co., Inc., c.1965.
16. Jalufka, N. W.: *Laser-Powered MHD Generators for Space Application*. NASA TP-2621, 1986.
17. Maxwell, Craig D.; and Myrabo, Leik N.: Feasibility of Laser-Driven Repetitively-Pulsed MHD Generators. AIAA-83-1442, June 1983.

Report Documentation Page

1. Report No. NASA TP-2798		2. Government Accession No.		3. Recipient's Catalog No.	
4. Title and Subtitle Laser Production and Heating of Plasma for MHD Application				5. Report Date March 1988	
				6. Performing Organization Code	
7. Author(s) N. W. Jalufka				8. Performing Organization Report No. L-16373	
9. Performing Organization Name and Address NASA Langley Research Center Hampton, VA 23665-5225				10. Work Unit No. 506-41-41-02	
				11. Contract or Grant No.	
12. Sponsoring Agency Name and Address National Aeronautics and Space Administration Washington, DC 20546-0001				13. Type of Report and Period Covered Technical Paper	
				14. Sponsoring Agency Code	
15. Supplementary Notes					
16. Abstract Laboratory experiments have been made on the production and heating of plasmas by the absorption of laser radiation. These experiments were performed in order to ascertain the feasibility of using laser-produced or laser-heated plasmas as the input for a magnetohydrodynamic (MHD) generator. Such a system would have a broad application as a laser-to-electricity energy converter for space power transmission. Experiments with a 100-J-pulsed CO ₂ laser were conducted to investigate the breakdown of argon gas by a high-intensity laser beam, the parameters (electron density and electron temperature) of the plasma produced, and the formation and propagation of laser-supported detonation (LSD) waves. Experiments were also carried out using a 1-J-pulsed CO ₂ laser to heat the plasma produced in a shock tube. The shock-tube hydrogen plasma reached electron densities of approximately 10 ¹⁷ cm ⁻³ and electron temperatures of approximately 1 eV. Absorption of the CO ₂ laser beam by the plasma was measured, and up to approximately 100-percent absorption was observed. Measurements with a small MHD generator showed that the energy extraction efficiency could be very large with values up to 56 percent being measured. These results strongly suggest that laser-driven MHD generators are viable candidates for application as laser-to-electricity converters in a space power transmission system.					
17. Key Words (Suggested by Authors(s)) Magnetohydrodynamics (MHD) Power generation Space power Plasma Laser-plasma interaction				18. Distribution Statement Unclassified—Unlimited Subject Category 75	
19. Security Classif.(of this report) Unclassified		20. Security Classif.(of this page) Unclassified		21. No. of Pages 9	
				22. Price A02	